PHY224 Interferometer

Turki Almansoori, Rui Geng

Due March 23rd, 2025

1 Abstract

Quantum mechanics demonstrates the wave-particle duality of light, notably through interference patterns. This study employs a Michelson interferometer with a green LED laser to determine three physical quantities: the laser's wavelength, the refractive index of a plastic prism, and the thermal expansion coefficient of aluminium. Measurements involved counting interference fringes resulting from precise adjustments of experimental parameters. Data analysis was conducted using Python's SciPy library for curve fitting and reduced chi-squared (χ_r^2) evaluations of the quality of fits.

We measured the laser wavelength as $533, \text{nm} \pm 8, \text{nm}$ ($\chi_r^2 = 0.26$), aligning closely with the manufacturer's specification ($532, \text{nm} \pm 1, \text{nm}$). For the refractive index, the plastic prism's rotation-induced fringe changes yielded $n = 1.604 \pm 0.005$ ($\chi_r^2 = 0.25$), consistent with literature values (1.4–1.7). Finally, the aluminium rod's thermal expansion resulted in a coefficient of $\alpha = 22.7 \times 10^{-6}/^\circ C \pm 0.2 \times 10^{-6}/^\circ C$ ($\chi_r^2 = 1.29$), closely matching the theoretical value ($23 \times 10^{-6}/^\circ C$). These results confirm the accuracy and reliability of our experimental setup.

2 Introduction and Theory

A Michelson interferometer divides incident light with a beam splitter and recombines it with a path difference, creating an interference pattern. As the path difference changes, fringe counts (N) vary accordingly. We can deduce the wavelength of green light[1] using:

$$N = \frac{2}{\lambda}\Delta x \tag{1}$$

where Δx is the change in distance (in μm unless stated otherwise). We will measure N and Δx, then use Python for curve fitting to estimate the wavelength λ.

To find the index of refraction (n) of a plastic prism, we place it between the beam splitter and mirror, vary the angle θ (measured in degrees, then converted to radians), and measure N. Using a small-angle approximation:

$$N \simeq \frac{t}{\lambda}\theta^2 \left(1 - \frac{1}{n}\right), \tag{2}$$

where t is the prism thickness (in mm, unless specified otherwise). Again, we measure N against θ and fit the resulting data to estimate n.

[1] Though the handout mentions red LEDs, our TA removed that portion.

We also measured the thermal expansion by attaching a mirror to an aluminum rod and heating it. The rod's expansion changes the path length, which we tracked via fringe counts:

$$N \simeq \frac{2L_0}{\lambda}\alpha\Delta T, \tag{3}$$

where L_0 is the rod's length at base temperature (in unit of mm), ΔT is the temperature change (in unit of ^oC), and α is the thermal expansion coefficient. Since ΔT is small, a linear approximation holds.

Because the setup is sensitive, random errors from noise and vibration would introduce larger uncertainties.[2]

3 Methods

3.1 Equipments

1. Laser (Thorlabs CPS532-C2) + Laser holder (Thorlabs KM100)
2. Lens (Thorlabs LMR1)
3. Beam splitter (Thorlabs CCM1-BS013, 400-700nm, 50:50)
4. Screen (Thorlabs EDU - VS1)
5. Adjustable mirror (Thorlabs KM100)
6. Movable mirror (Thorlabs SM1ZP)
7. Rotation mount (Thorlabs PR01 Rotation Mount)
8. Vernier Caliper (IGaging EZCal IP54)
9. Plastic Prism
10. Aluminium rod with mirror (Thorlabs K-102 E3218)
11. Ruler
12. Thermometer (Greisinger G1710)
13. Aluminium rod holder (Thorlabs BA1S)
14. Power Supply.

3.2 Setups

The core setup involves a laser, a beam splitter, a lens, and two mirrors, as well as a screen to project the interference pattern onto. We have three slightly different experimental setups (one for each exercise). The positions of the laser, lens, beam splitter, adjustable mirror, and screen are kept the same for all exercises.

[2]See Appendix for generic and model-specific propagation formulas.

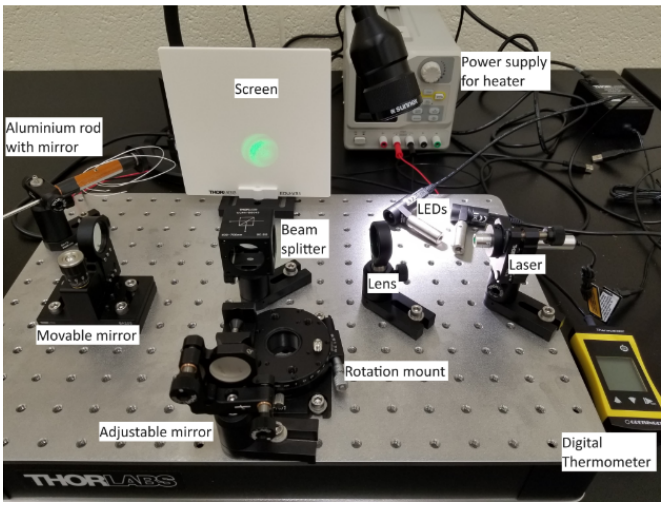

Figure 1: The lab was set up according to the Interferometry manual. Picture source: the manual.

For the wavelength measurement, we place an adjustable mirror and a movable mirror around a beam splitter. We vary the micrometer dial, Δx, causing fringes to appear or disappear. We found it simpler to count about five fringes (N) every time and record the dial's movement. From (1), a linear plot lets us solve for the empirical wavelength, λ.

For the index of refraction, we keep the same setup but add a plastic prism clamped to a rotation mount between the adjustable mirror and the beam splitter. We measure its thickness t with a vernier caliper, use λ from our wavelength result, and record the change in N for each rotation angle θ. Using (2), we then fit the data to predict n.

For thermal expansion, we replace the movable mirror with an aluminum rod (plus a mirror) connected to a power supply. We record temperature changes, ΔT, count fringe changes (N), and use (3) with the rod's base temperature length L_0 and our measured λ to find the thermal expansion coefficient α.

Note: We sum fringe counts cumulatively (i.e. at index $i \geq 1$, $dN_{\text{new}}[i] = dN_{\text{new}}[i-1]+dN_{\text{old}}[i]$) and propagate uncertainties additively ($u_{\text{new}}(x_i) = \sqrt{u_{\text{new}}(x_{i-1})^2 + u_{\text{old}}(x_i)^2}$).

Further note: uncertainty propagation for the prediction models are in the Appendix section.

4 Results, Plots, Uncertainties and Analysis

4.1 Wavelength

4.1.1 Data gathering's systematic error

Because fringe counting relies on human observation, we suspected a systematic error when our measured wavelength deviated by over $100nm$ from the manufacturer's specification. Despite TA consultations and hardware adjustments, the discrepancy remained. Post-measurement analysis showed we consistently miscounted each measurement's fringe by one, likely due to the rapid changes when touching or releasing the turning knob. We corrected our data accordingly and used this adjusted wavelength for subsequent analyses. We also excluded the zero-fringe data point to avoid division-by-zero errors in our uncertainty calculations.

4.1.2 Wavelength Curve Fitting

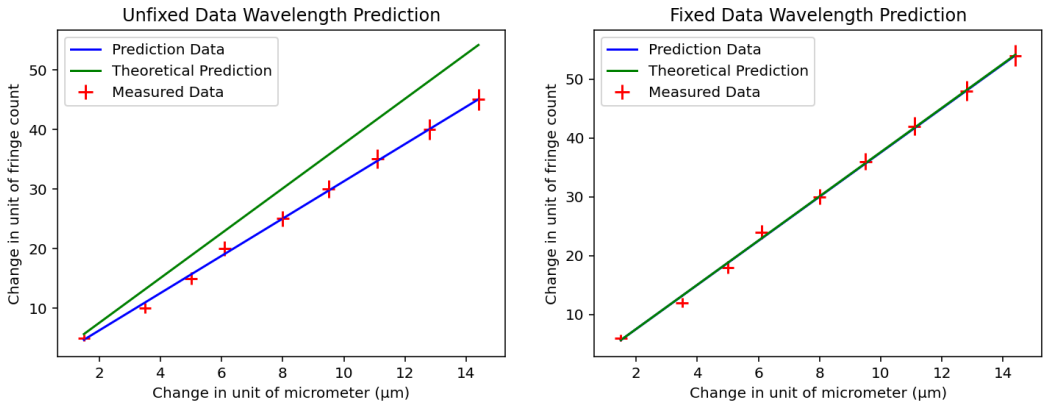

Figure 2: Comparison of Unfixed and Fixed data plots of the wavelength prediction. Fixed data prediction model: $N = \frac{2}{533\times10^{-9}m}\Delta x$. *Theoretical model uses the laser's manufacturer spec wavelength of* $532nm$, *expressed as* $N = \frac{2}{532\times10^{-9}m}\Delta x$

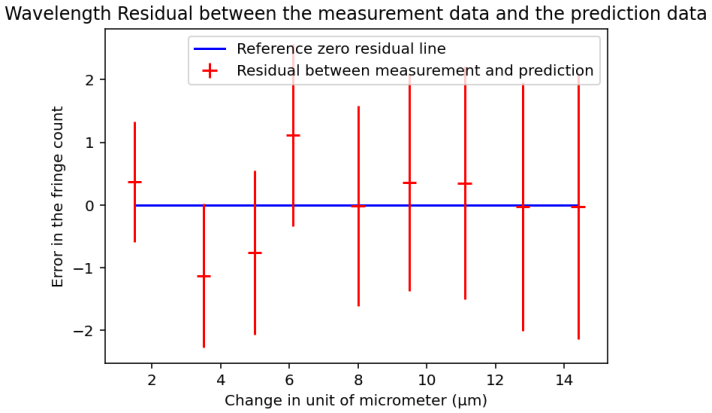

Figure 3: Residual Plot of the prediction data versus the measured data.

For the above plots, we applied the curve fitting function to the fixed/adjusted dataset. We obtained our fitted parameter to be:

$$\lambda \approx 533nm \pm 8nm$$

Using this predicted parameter, our model can then be expressed as:

$$N = \frac{2}{533 \times 10^{-9}m}\Delta x \tag{4}$$

Then, after propagating the model's uncertainty, our reduced chi square value was calculated to be:

$$\chi_r^2 \approx 0.26$$

This χ_r^2 is less than 1, indicating that the model is overfitting the measurement data. Especially considering that the data exhibited a very linear behaviour, to the point the prediction values are almost, if not always, within the uncertainty's range. Interestingly, this phenomenon does not change regardless of the dataset being adjusted or not, as can be seen in the comparison plots.

4.2 Index of Refraction

From this section onward, we will discuss the prediction parameters and analysis before demonstrating the relevant plots. By applying the curve fitting function to our measurement dataset, we obtained the prediction parameter (index of refraction) to be:

$$n \approx 1.603 \pm 0.005$$

Using our measured thickness ($t = 7.70mm \pm 0.03mm$)[3], and previously predicted wavelength ($\lambda \approx 533nm \pm 8nm$), our prediction model can then be written as:

$$N \simeq \frac{7.7 \times 10^{-3}m}{533 \times 10^{-9}m}\theta^2 \left(1 - \frac{1}{1.603}\right) \tag{5}$$

We also obtained the reduced chi square value[4] to be:

$$\chi_r^2 \approx 0.25$$

Similar to the wavelength fit, our index-of-refraction model also has $\chi_r^2 < 1$, suggesting overfitting. The fit closely follows all data points, and we see no simple way to reduce this effect without arbitrarily modifying our uncertainties or model. We thus compared our result, $n \approx 1.603 \pm 0.005$, to a standard plastic range of 1.4–1.7.[5] Despite the overfitting, our prediction lies within this interval, indicating a relatively reasonable estimate for the plastic's refractive index.
Plots for the index of refraction prediction:

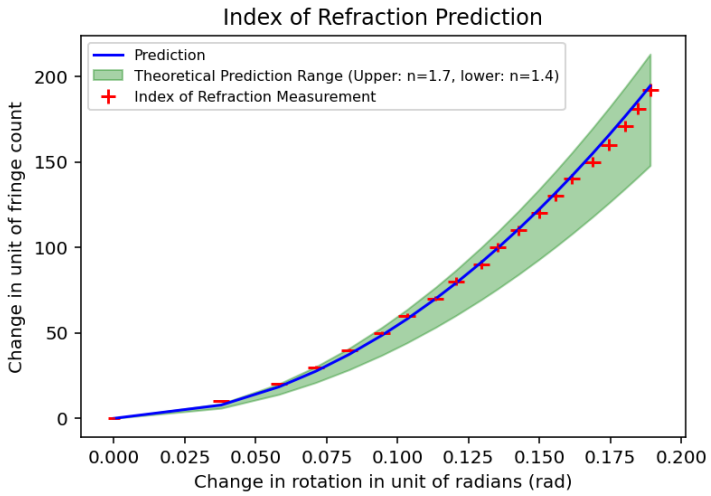

Figure 4: Plot of the index of refraction. Prediction model: $N \simeq \frac{7.7\times10^{-3}m}{533\times10^{-9}m}\theta^2\left(1-\frac{1}{1.603}\right)$. *Theoretical prediction range uses the same equation, but with the laser's manufacturer spec wavelength of* $532nm$*, an upper range of index of refraction* $n = 1.7$*, and a lower range of* $n = 1.4$.

[3]Value is average from all measurements, uncertainty propagated using formula in Appendix, based on data std and device accuracy of 0-6"/0.001".

[4]See the Appendix section for the formula.

[5]Wikipedia: `https://en.wikipedia.org/wiki/Refractive_index`, retrieved March 20, 2025.

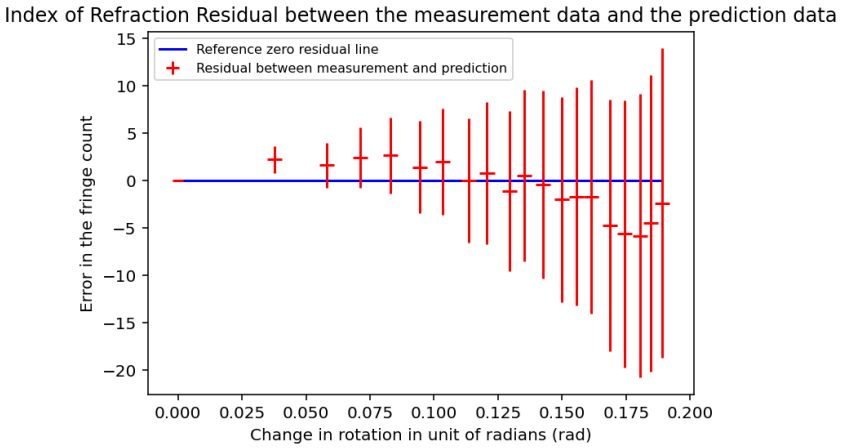

Figure 5: Residual Plot of the prediction data versus the measured data.

4.3 Thermal Expansion Coefficient of Aluminium

Using curve fitting function, we predicted the thermal expansion coefficient of aluminium to be:

$$\alpha \approx 22.7 \times 10^{-6}/^{o}C \pm 0.2 \times 10^{-6}/^{o}C$$

Using our base temperature length of the aluminium rod ($L_0 = 90.12mm \pm 0.02mm$) and our previously predicted wavelength ($\lambda \approx 533nm \pm 8nm$), our prediction model can then be specified as:

$$N \simeq \frac{2 \times 0.09012m}{533 \times 10^{-9}m}(22.7 \times 10^{-6}/^{o}C)\Delta T \tag{6}$$

Then having propagated the model's uncertainties, we obtained a reduced chi square value of:

$$\chi_r^2 \approx 1.29$$

This χ_r^2 value is slightly above 1, indicating that while our prediction model is relatively accurate, it might be slightly underfitting the dataset. We can also observe in the following plots, that as temperature kept increasing, the data points started to deviate from exhibiting a linear expression. We hypothesize that, although with limited confidence, possible reasons might be due to: measuring error (such as: blurry vision due to eyesight problems), or reaching the temperature warning stated in the lab PDF[6]. However, more knowledge is required to make a more adequate reasoning to this deviation.

The plots for the thermal expansion coefficient prediction are as follow:

[6] "The thermal expansion of aluminium is sufficiently small that your data should be linear unless you get to temperatures hot enough to risk melting things (please don't melt anything)", page 6 of manual.

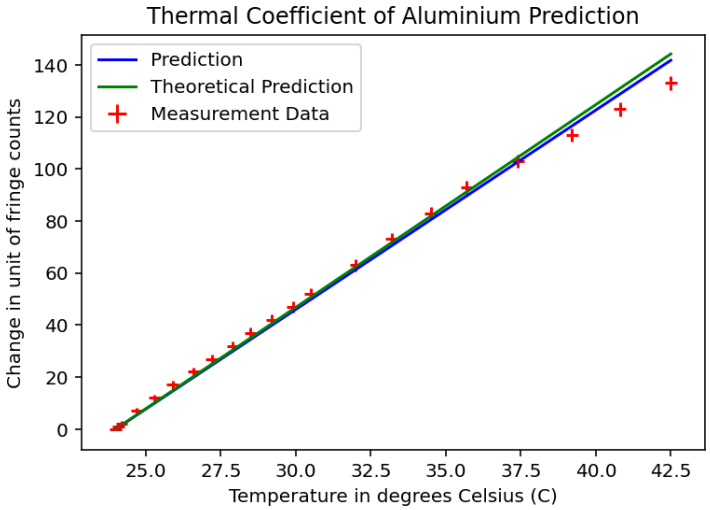

Figure 6: Plot of the thermal expansion coefficient of aluminium. Prediction model: $N \simeq \frac{2\times 0.09012m}{533\times 10^{-9}m}(22.7\times 10^{-6}/^oC)\Delta T$. *The theoretical prediction uses the manufacturer spec wavelength of* $532nm$ *and thermal expansion coefficient of aluminium* $\alpha = 23\times 10^{-6}/^oC$.

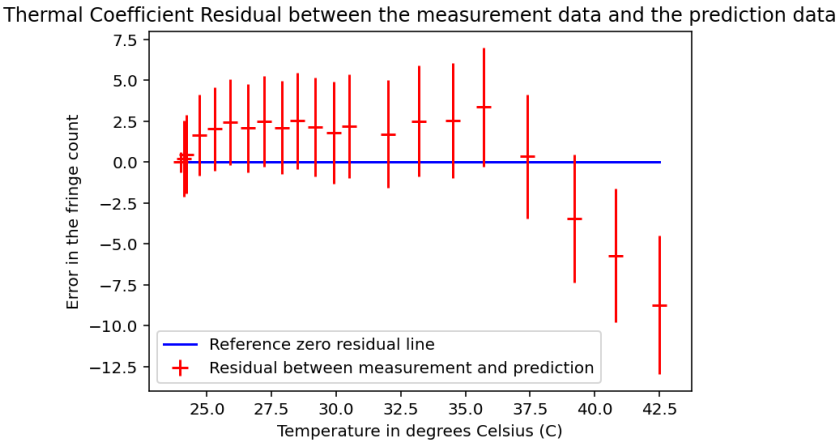

Figure 7: Residual Plot of the prediction model data versus the measured data.

5 Conclusion

Through systematic measurements with a Michelson interferometer, we derived three key physical parameters—laser wavelength, plastic prism index of refraction, and the thermal expansion coefficient of aluminum. After correcting a systematic fringe-counting error and excluding a zero-fringe data point, the fitted wavelength ($533nm\pm 8nm$) agreed well with the device's specified wavelength of $532nm\pm 1nm$. Our plastic prism's fitted refractive index (1.603 ± 0.005) fell within the known range for typical plastics (1.4–1.7). Finally, the fitted thermal expansion coefficient of aluminum ($22.7\times 10^{-6}/^oC\pm 0.2\times 10^{-6}/^oC$) matched its accepted value ($23\times 10^{-6}/^oC$) reasonably close.

Reduced chi-squared values indicated minor over- or underfitting in certain datasets; however, the predictions remained within physically reasonable ranges. Systematic deviations were attributed to inherent measurement limitations (rapid fringe shifts), while deviations in the data points were due to the sensitivity of the setup (due to outside noise) and error propogation. Overall, the strong agreement with manufacturer specifications and published values confirms both the reliability of the interferometer setup and the accuracy of our methods and data analysis.

6 Appendix

6.1 Uncertainty Propagation - Wavelength Prediction

$$N_w = \frac{2}{\lambda}\Delta x$$
$$u(2\Delta x) = 2u(\Delta x)$$
$$u(N_w) = (\frac{2}{\lambda}\Delta x)\sqrt{\left(\frac{u(\lambda)}{\lambda}\right)^2 + \left(\frac{2u(\Delta x)}{2\Delta x}\right)^2}$$

6.2 Uncertainty Propagation - Index of Refraction Prediction

$$N_i \simeq \frac{t}{\lambda}\theta^2\left(1-\frac{1}{n}\right)$$
$$u\left(\frac{t}{\lambda}\right) = \left(\frac{t}{\lambda}\right)\sqrt{\left(\frac{u(t)}{t}\right)^2 + \left(\frac{u(\lambda)}{\lambda}\right)^2}$$
$$u(\theta^2) = 2\theta^2\frac{u(\theta)}{\theta} = 2\theta u(\theta)$$
$$u\left(1-\frac{1}{n}\right) = \frac{u(n)}{n^2}$$
$$u\left(\frac{t}{\lambda}\theta^2\right) = \frac{t}{\lambda}\theta^2\sqrt{\left(\frac{u\left(\frac{t}{\lambda}\right)}{\frac{t}{\lambda}}\right)^2 + \left(\frac{u(\theta^2)}{\theta^2}\right)^2}$$
$$u(N_i) = \frac{t}{\lambda}\theta^2\left(1-\frac{1}{n}\right)\sqrt{\left(\frac{u\left(\frac{t}{\lambda}\theta^2\right)}{\frac{t}{\lambda}\theta^2}\right)^2 + \left(\frac{u\left(1-\frac{1}{n}\right)}{1-\frac{1}{n}}\right)^2}$$

6.3 Uncertainty Propagation - Thermal Expansion Coefficient Prediction

$$N_t \simeq \frac{2L_0}{\lambda}\alpha\Delta T$$
$$u\left(\frac{2L_0}{\lambda}\right) = \frac{2L_0}{\lambda}\sqrt{\left(\frac{u(L_0)}{L_0}\right)^2 + \left(\frac{u(\lambda)}{\lambda}\right)^2}$$
$$u(\alpha\Delta T) = \alpha\Delta T\sqrt{\left(\frac{u(\alpha)}{\alpha}\right)^2 + \left(\frac{u(\Delta T)}{\Delta T}\right)^2}$$
$$u(N_i) = \frac{2L_0}{\lambda}\alpha\Delta T\sqrt{\left(\frac{u\left(\frac{2L_0}{\lambda}\right)}{\frac{2L_0}{\lambda}}\right)^2 + \left(\frac{u(\alpha\Delta T)}{\alpha\Delta T}\right)^2}$$

6.4 Generic Uncertainty Propagation

For y being the measurand with inputs $x_i, \forall i \in 1, ...$:

$$u(y) = \sqrt{\left(\frac{\partial y}{\partial x_1}\right)^2 (u(x_1))^2 + \left(\frac{\partial y}{\partial x_2}\right)^2 (u(x_2))^2 + \dots}$$

6.5 Reduced Chi Square Value χ_r^2 Calculation:

For d = degree of freedom, where d = (number of datapoint - number of fitted parameters). x_i is the independent variable, and y_i is the dependent variable of the i^{th} measurement, and $f(x_i)$ = predicted value using the x_i variable. Finally u_i is the propagated uncertainty for the model.

$$\chi_r^2 = \frac{1}{d}\sum_{i=1}^{N}\left(\frac{y_i - f(x_i)}{u_i}\right)^2$$